Journal of Atmospheric and Solar-Terrestrial Physics 188 (2019) 52–61

Contents lists available at ScienceDirect

Journal of Atmospheric and Solar-Terrestrial Physics

journal homepage: www.elsevier.com/locate/jastp

Evaluation of some rain attenuation prediction models for satellite communication at Ku and Ka bands

K.C. Igwe[a,*], O.D. Oyedum[a], M.O. Ajewole[b], A.M. Aibinu[c]

[a] *Department of Physics, Federal University of Technology, Minna, Nigeria*
[b] *Department of Physics, Federal University of Technology, Akure, Nigeria*
[c] *Department of Mechatronics Engineering, Federal University of Technology, Minna, Nigeria*

ARTICLE INFO

Keywords:
Elevation angle
Ka-band
Ku-band
Rain attenuation
Rain rate

ABSTRACT

Propagation of radio waves between terrestrial and earth-space links at frequencies above 10 GHz are adversely affected by weather, especially rain. Rain-induced attenuation is an important propagation effect that has to be considered in satellite communication system design. Prediction of rain attenuation for earth-space links in North Central Nigeria at Ku and Ka bands is investigated using five rain attenuation models: The ITU-R P.618 model, Bryant model, Garcia-Lopez model, Svjatogor model and Simple attenuation model (SAM). The main objective is to determine the optimal rain attenuation prediction models for satellite communication in this region. 33 years (1983–2015) daily rainfall data obtained from the Nigerian Meteorological Agency (NIMET) were used. Three elevation angles were considered: 55° 42.5° and 23°. The results obtained showed that the ITU-R P.618, Garcia-Lopez and Bryant models performed best in this region. Also, attenuation ranged from 14 dB to 16 dB at 55° elevation angle, 15 dB–16 dB at 42.5° elevation angle and 20 dB–22 dB at 23° elevation angle for exceedance time percentage of 0.01% at Ku-band in all the stations. For the Ka-band, attenuation varied between 33 dB and 37 dB at 55° elevation angle, 33 dB and 37 dB at 42.5° elevation angle and between 42 dB and 48 dB at 23° elevation angle for same 0.01% exceedance time percentage. From the values of rain attenuation predicted for 0.01% time exceedance, availability of signal is possible at 42.5° and 55° elevation angles but impossible at 23° elevation angle at Ku-band. At Ka-band, the predicted rain attenuation values for 0.01% time exceedance have shown that availability of signal is impossible at all three elevation angles, which implies total signal fade out during such rainfall events in the region.

1. Introduction

The ever increasing demand for communication systems by consumers and professionals alike has resulted in congestion of the lower frequency bands (≤ 6 GHz). This has thus necessitated the exploration and consequent migration to higher frequency bands (11 GHz - 30 GHz) in order to meet the high demand for quality communication service (Kestwal et al., 2014; Shrestha and Choi, 2018). However, these higher frequency bands (Ku and Ka bands in this case), though reliable and efficient for satellite communication, have their challenges. The major threat to reliability and efficiency here is rain-induced degradation. Impairments by other atmospheric factors such as cloud, fog, ice, hail, snow and atmospheric gases occur, but signal degradation by rain is more severe in comparison (Crane, 2003; Mandeep, 2011; Shrestha et al., 2016; Shrestha and Choi, 2017; Hossain and Islam, 2017), hence the need for careful and detailed study of the effects of rain-induced attenuation on system availability and performance in these frequency bands.

The severity of rain impairment increases with frequency and also varies with geographical locations (Choi et al., 1997). The frequency attenuated can be higher than 10 GHz for the temperate region, while it can be as low as 7 GHz in the tropical/equatorial regions because of the higher rainfall intensity and larger raindrops experienced in the latter (Moupfouma, 1984; Moupfouma and Martin, 1995; Ojo et al., 2008). The attenuation that results from absorption by rain drops is larger than the attenuation from scatter at smaller wavelengths in comparison to the drop size, while the attenuation resulting from scatter is more enormous than losses resulting from absorption for wavelengths that are longer in comparison to the rain drop size (Tamosiunaite et al., 2010). Rain attenuation depends on rain rate, terminal velocity, size

* Corresponding author.
E-mail addresses: k.igwe@futminna.edu.ng (K.C. Igwe), onyedidavid@futminna.edu.ng (O.D. Oyedum), oludare.ajewole@futa.edu.ng (M.O. Ajewole), abiodun.aibinu@futminna.edu.ng (A.M. Aibinu).

https://doi.org/10.1016/j.jastp.2019.03.005
Received 25 November 2018; Received in revised form 19 February 2019; Accepted 11 March 2019
Available online 14 March 2019
1364-6826/

distribution and shape of the raindrops (Sujimol et al., 2015). Although, attenuation due to rain can be accurately measured by the use of satellite beacon signals and radiometers, but since such propagation experiments are carried out only in very few places and for a limited number of frequencies and link geometry in the world, results obtained cannot be directly applied to all locations. Hence, various attenuation models based on empirical facts and the use of available meteorological data have been developed to provide enough inputs for system margin calculations in every region of the world (COST 225, 2002). This implies that accurate prediction of rain-induced attenuation on propagation paths is imperative when planning both microwave and terrestrial line-of-sight system links (Salonen and Poiares-Baptista, 1997).

High rainfall intensity is difficult to be recorded and measured experimentally; it is also highly variable from year to year. In systems design, it is the highest rainfall rates that are of great interest and short integration time rainfall is the most essential input parameter in the prediction models for rain attenuation (Salonen and Poiares-Baptista, 1997).

Two broad classes of rain attenuation prediction on any microwave link can be considered: The analytical models which are based on physical laws governing electromagnetic wave propagation, and which attempt to reproduce the actual physical behaviour in the attenuation process; and the empirical models which are based on measurement databases from stations in different climatic zones within a given region. However, when a physical approach is used, not all the input parameters needed for the analysis are available. Therefore, empirical method is the most used methodology (Crane, 2003; Ramachandran and Kumar, 2005).

In Nigeria, the Nigerian Communication Satellite (NIGCOMSAT-1R) which was launched in 2011, as well as other satellite outfits like INTELSAT, EUTELSAT, ASTRA and NSS7 which are linked to various digital television stations like DStv, HiTv, Multi Tv and MyTv Africa operate on Ku and Ka bands. Therefore, knowledge of the degree of rain-induced degradation in different locations within the region is imperative so as to guide satellite engineers and scientists on improving the quality of local communication networks.

This paper therefore investigates the degree of rain-induced attenuation on satellite communication in Central Nigeria by evaluating the optimal predicting models. Results obtained will be beneficial to operators and intended consumers of services from various satellite outfits, especially the NIGCOMSAT-1R.

2. Background

Several rain rate models have been developed for predicting rainfall rate. Amongst the different models that have been used are the Crane (1985), Segal (1986) and Watson (Watson et al., 1981); but all these have their various drawbacks, from inaccurate results for other parts of the world other than the United States (as in the case of Crane model), to low spatial resolution of point measurements on a global scale (as in Watson model). Others include the Rice-Holmberg (Rice and Holmberg, 1973) and the Moupfouma and Martin (Moupfouma and Martin, 1995) models. The drawback of the Rice-Holmberg model is its cumbersome design because of certain parameters required: 30 years maximum monthly rainfall accumulation, thunderstorm ratio (the ratio of thunderstorm rain to total rain in a given location) and the average annual rainfall accumulation. The thunderstorm ratio is usually not available from local weather stations. Also, the Rice-Holmberg method has been found to overestimate rain rates in the high availability range (0.01%) and underestimate rain rates between 0.1% and 1% (Ojo et al., 2008).

The Moupfouma and Martin model has been observed to be suitable for tropical climates (Ajayi et al., 1996; Mandeep, 2004; Ojo et al., 2008, 2009), but its setback is that the point rainfall rate which is a very important input parameter is not always available. Hence Chebil's simple method (Chebil and Rahman, 1999) for point rainfall rate estimation is most preferable since the point rainfall rate (mm/h) which is the main input parameter used for the prediction of rain attenuation is estimated from the mean annual rainfall accumulation.

3. Analyses of experimental data

3.1. Rain rate

The Chebil model is expressed as:

$$R_{0.01}(mm/h) = \alpha M^{\beta} \tag{1}$$

where $R_{0.01}$ is the point rain intensity exceeded at time percentage of 0.01%, M is the mean annual accumulation of rain while α and β are regression coefficients given as 12.2903 and 0.2973 respectively. This simple approach by Chebil is most suitable for the type of data used in this research. This rain rate model has been widely used for the prediction of rainfall intensity all over the world (Ajayi et al., 1996; Emiliani et al., 2004; Ojo et al., 2009; Obiyemi et al., 2014).

3.2. Rain attenuation models

There are different rain attenuation models employed for the prediction of rain-induced attenuation for satellite-to-earth communication. Five of these models are selected and used in this work. These are the Simple Attenuation Model (Stutzman and Dishman, 1984), the Svjatogor model (Svjatogor, 1985), the Garcia-Lopez model (Garcia-Lopez et al., 1988), the Bryant model (Bryant et al., 1999) and the ITU-R P.618-9 model (ITU-R, 2007). These models are explained in details below.

3.2.1. Simple Attenuation Model

Stutzman and Dishman (1984) developed the Simple Attenuation Model (SAM) based on an effective rain rate profile that is exponential in shape. It incorporates the individual characteristics of the stratiform and convective types of rain. The SAM model is given as

$$A = \Upsilon \frac{1 - exp\left[-\Upsilon b ln\left(\frac{R_{\%p}}{10}\right)\right] L_S Cos\theta}{\Upsilon b ln\left(\frac{R_{\%p}}{10}\right) Cos\theta}; \quad R_{\%p} > 10\ mm/h \tag{2}$$

where L_S (km) is the slant path length given as

$$L_S(km) = \frac{H_r - H_s}{Sin\ \theta} \quad \theta \geq 5° \tag{3}$$

where H_r is the rain height and H_s is the station height. Θ (degrees) is the elevation angle between the horizontal projection and slant path, ϒ is the specific attenuation as given in ITU-R (2005) and the empirical constant, b = 1/14.

The rain height, H_r can be derived as:

$$H_r \begin{cases} H_o; & R \leq 10\ mm/h \\ H_o + log\left(\frac{R}{10}\right); & R > 10\ mm/h \end{cases} \tag{4}$$

H_o (km) is the 0° isotherm height. The seasonal mean of H_o is obtained by (Crane, 1978):

$$\begin{aligned} H_o &= 4.8 & |\lambda| \leq 30° \\ H_o &= 7.8 - 0.1|\lambda| & |\lambda| \geq 30° \end{aligned} \tag{5}$$

where λ is the latitude of the station.

3.2.2. Svjatogor attenuation model

Svjatogor (1985) derived an attenuation model whose effective rain height, H_r depends on the rain intensity. The rain height is given as

$$H_r(km) = \frac{2.7}{log_{10}(0.3R_p + 1.5)} + 0.0015R_p \tag{6}$$

The path length reduction factor is expressed as:

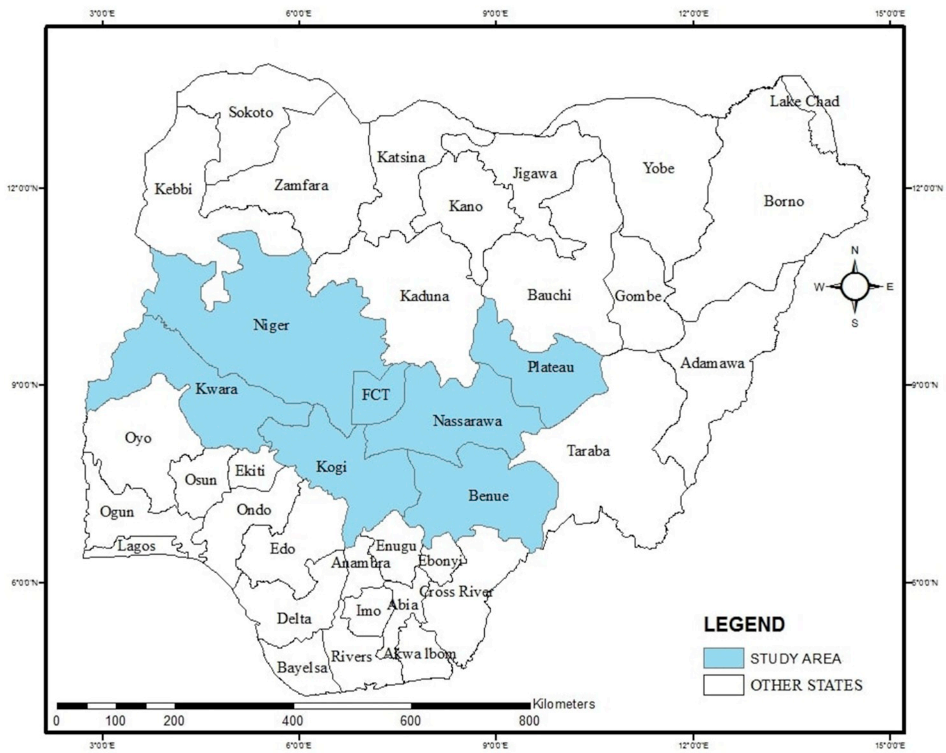

Fig. 1. The North Central region of Nigeria.

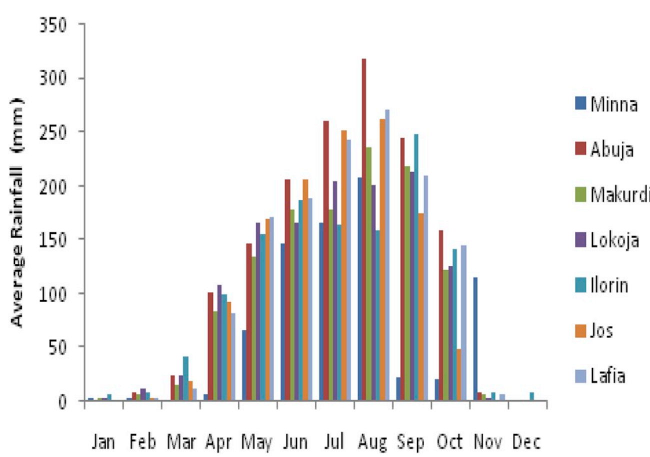

Fig. 2. 33 years average rainfall for the study area.

$$k_{rs} = e^{Y}; \quad Y = -0.0045R_p^{0.68}\left[\frac{H_R}{tan\theta}\right]^{0.6} \tag{7}$$

The rain attenuation is then given as

$$A(dB) = kR_p^{\alpha}L_s k_{rs} \tag{8}$$

where:

$$L_S(km) = \frac{H_r - H_s}{Sin\ \theta} \quad \text{for } \theta \geq 5^{\circ} \tag{9}$$

$$L_S(km) = \frac{2(H_r - H_s)}{\left[sin^2\theta + \frac{2(H_r - H_s)}{R_e}\right]^{1/2} + sin\theta} \quad \text{for } \theta < 5^{\circ} \tag{10}$$

R_e is the effective radius of the earth. It is taken as 8500 km.

3.2.3. The Garcia-Lopez attenuation model

Garcia-Lopez et al. (1988) developed a simple method for the prediction of rain attenuation on satellite radio links which is an extension of that proposed for terrestrial links. Values of coefficients considered during calculation of the attenuation are separate for tropical regions. This method is given by

$$A = \frac{kR^{\alpha}L_s}{\left[a + \left\{\frac{L_s(bR + cL_s + d)}{e}\right\}\right]} \tag{11}$$

where R is the point rainfall rate in mm/h, coefficients k and α are constants determined based on frequency, polarisation and elevation angle as given by ITU-R (2005). a, b, c and d are constants depending

Table 1
Station characteristics for north central region.

Station	Lat (°N)	Long (°E)	Elevation (m)	Annual rain (mm)	$R_{0.01}$ (mm/h)
Minna	9.54	6.54	249	1201	103.2
Abuja	9.00	7.28	334	1457	109.4
Makurdi	7.70	8.50	142	1179	102.7
Lokoja	7.47	6.44	204	1229	103.9
Ilorin	8.32	4.34	304	1232	104.0
Jos	9.58	8.57	1110	1239	104.2
Lafia	8.50	8.47	403	1339	106.7

Table 2
Geometric features of satellite links at 55° by ITU-R model.

Station	Rain Height (km)	Slant Path Length, L_S (km)	Horizontal Projection, L_G (km)	Effective Path Length, L_E (km)	
				Ku-mid (f = 12.675)	Ka-mid (f = 19.45)
Minna	4.79	5.54	3.18	3.01	3.52
Abuja	4.76	5.40	3.10	2.88	3.38
Lokoja	4.75	5.55	3.18	3.03	3.54
Makurdi	4.76	5.64	3.23	3.07	3.59
Jos	4.76	4.45	2.55	2.69	3.13
Ilorin	4.78	5.46	3.13	2.99	3.50
Lafia	4.77	5.33	3.06	2.91	3.41

Table 3
Geometric features of satellite links at 42.5° by ITU-R model.

Station	Rain Height (km)	Slant Path Length, L_S (km)	Horizontal Projection, L_G (km)	Effective Path Length, L_E (km)	
				Ku-mid (f = 12.675)	Ka-mid (f = 19.45)
Minna	4.79	6.72	4.95	3.04	3.52
Abuja	4.76	6.55	4.83	2.90	3.38
Lokoja	4.75	6.73	4.96	3.06	3.55
Makurdi	4.76	6.84	5.04	3.11	3.60
Jos	4.76	5.40	3.98	2.74	3.15
Ilorin	4.78	6.63	4.88	3.03	3.51
Lafia	4.77	6.46	4.77	2.95	3.42

Table 4
Geometric features of satellite links at 23° by ITU-R model.

Station	Rain Height (km)	Slant Path Length, L_S (km)	Horizontal Projection, L_G (km)	Effective Path Length, L_E (km)	
				Ku-high (f = 12.675)	Ka-mid (f = 19.45)
Minna	4.79	11.61	10.69	4.15	4.57
Abuja	4.76	11.33	10.43	3.98	4.39
Lokoja	4.75	11.63	10.71	4.20	4.61
Makurdi	4.76	11.82	10.88	4.27	4.68
Jos	4.76	9.33	8.59	3.74	4.08
Ilorin	4.78	11.46	10.54	4.15	4.55
Lafia	4.77	11.18	10.29	4.04	4.44

on the geographical area and can be easily determined by regression techniques based on simultaneous rain intensity and rain attenuation plots. Coefficient e is a scaling factor and by taking $e = 10^4$, worldwide coefficients are: a = 0.7, b = 18.35, c = −16.51 and d = 500 (COST 225, 2002). For tropical climates, a = 0.72, b = 7.6, c = −4.75 and d = 2408 (Panchal and Joshi, 2016). L_s (km) is the slant path up to the rain height and it is as given in equation (3).

The rain height H_r is given as:

$$H_r(km) = \begin{cases} 4 & 0 < \Psi < 36^\circ \\ 4 - 0.075(|\Psi| - 36^\circ) & \Psi \geq 36^\circ \end{cases} \tag{12}$$

where Ψ is the latitude of the earth station in degrees.

3.2.4. Bryant attenuation model

The Bryant attenuation model (Bryant et al., 1999) was derived based on the use of the concept of effective rain cell and variable rain height to calculate the distribution of rain attenuation. The following steps are employed in the calculation:

Step 1: calculate the PR parameter:

$$PR = 1 + \frac{2}{\pi}\frac{L}{D} \tag{13}$$

where D is the rain cell diameter given by

$$D = 540(R_p^{-12}) \tag{14}$$

where R_p is the point rainfall rate exceeded at p percentage of time and L is the horizontal projection given by

$$L = \frac{H_r}{tan\theta} \tag{15}$$

Step 2: calculate the rain height, H_r:

$$H_r(km) = 4.5 + 0.0005R_p^{1.65} \tag{16}$$

Step 3: calculate the attenuation along the slant path:

$$A = 1.57D_m k_n \Upsilon_p \frac{L_S}{\xi L + D} \tag{17}$$

where: L_S is the slant-path length.

Υ_p (dB/km) is the specific attenuation

$$D_m = \left(\frac{2}{\pi}\right)D$$

k_n is the number of cells and it is given as

$$k_n = \exp(0.007R_p) \tag{18}$$

$$\xi = \begin{cases} \frac{1}{\sqrt{2}}\exp(sin\theta) & \theta \leq 55^\circ \\ 1.1tan\theta & \theta > 55^\circ \end{cases} \tag{19}$$

3.2.5. The ITU-R P. 618-9 model

This model uses rain rate at 0.01% probability level for the estimation of attenuation and then applies an adjustment factor for the predicted rain attenuation depth for other probabilities.

The steps required for the analysis are given below:

Step 1: Determine the rain height, H_R as:

$$H_R = h_o + 0.36 \text{ km} \tag{20}$$

where h_o is the 0 °C isotherm height above mean sea level of the location.

Step 2: Determine the slant path length L_s, below the rain height from:

$$L_S = \frac{H_R - H_S}{Sin\ \theta} \tag{21}$$

where θ is the elevation angle and H_S is the height of the location above sea level.

Step 3: Obtain the horizontal projection, L_G, of the slant path length from:

$$LG = LS \text{ Cos}\theta \tag{22}$$

Step 4: Obtain the point rainfall rate, $R_{0.01}$ (mm/h) exceeded for 0.01% of an average year from one-minute integration rain rate data for the location

Step 5: Obtain the Specific attenuation, $\gamma_{R0.01}$ (dB/km) for 0.01% of time as given by:

$$\gamma_{R0.01} = kR_{0.01}^{\alpha} \tag{23}$$

where parameters k and α are determined as functions of frequency in GHz as given in ITU-R P.838–3 (ITU-R, 2005).

Step 6: Calculate the horizontal reduction factor, $r_{h0.01}$ for 0.01% of time using

$$r_{h0.01} = \frac{1}{1 + 0.78\sqrt{\left(\frac{L_G * \gamma_{R0.01}}{f}\right)} - 0.38\left[1 - \exp(-2L_G)\right]} \tag{24}$$

where f is the frequency in GHz.

Step 7: Calculate the vertical adjustment factor, $v_{0.01}$ (km):

$$L_R = \frac{L_G r_{0.01}}{\cos\theta} \text{ for } \rho > \theta \tag{25a}$$

Otherwise,

$$L_R = \frac{H_R - H_S}{\sin\theta},\ for\ \rho \leq \theta \tag{25b}$$

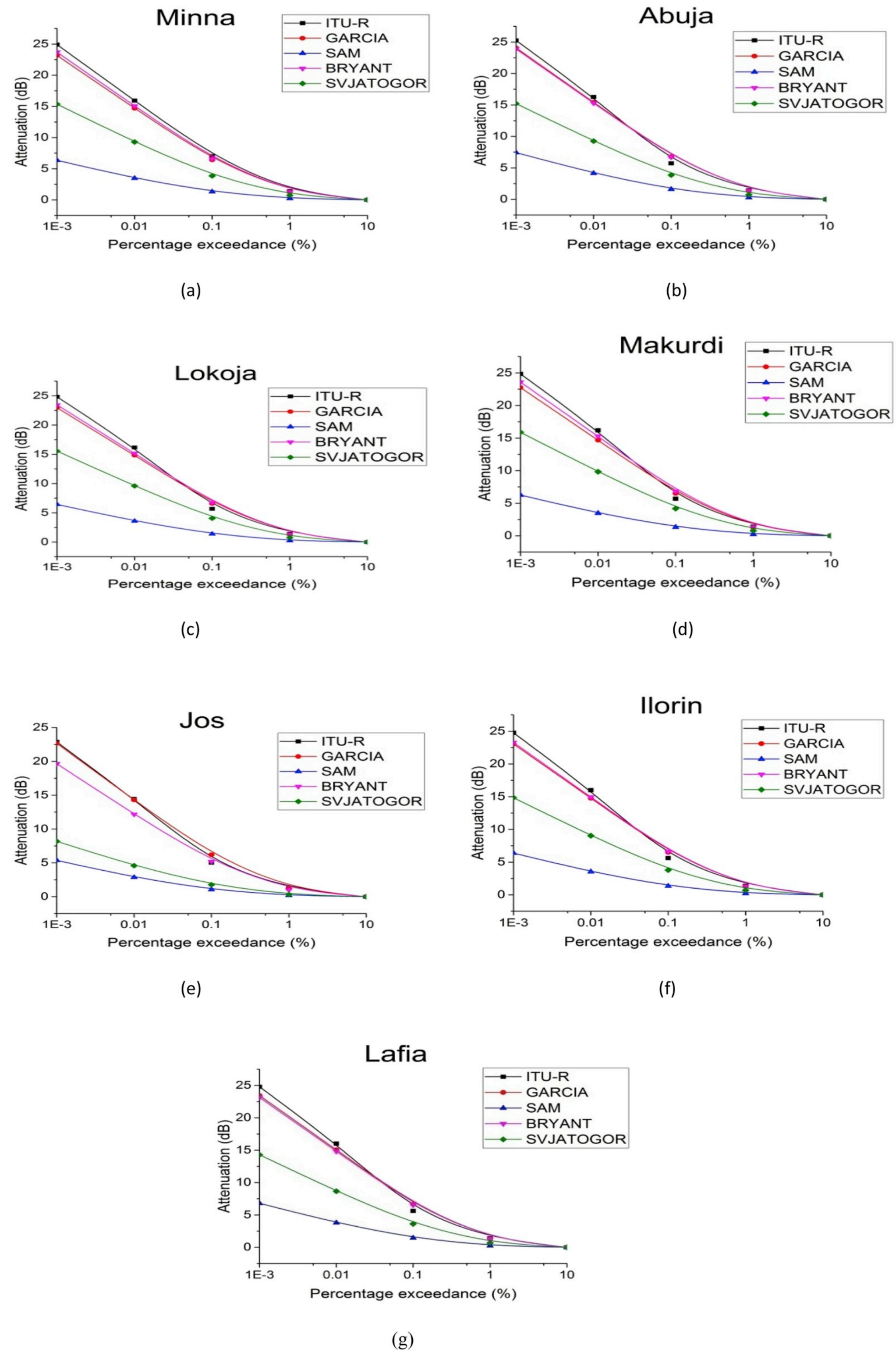

Fig. 3. Cumulative distribution of rain attenuation at 55° and Ku-band.

where

$$\rho = \tan^{-1}\left(\frac{H_R - H_S}{L_G r_{h0.01}}\right) \tag{25c}$$

therefore,

$$v_{0.01} = \frac{1}{1 + \sqrt{\sin\theta}\left[31\left(1 - \exp\left(-\frac{\theta}{[1+\sigma]}\right)\right)\frac{\sqrt{L_G\,\gamma_{R0.01}}}{f^2} - 0.45\right]} \tag{25d}$$

where

$\sigma = 36 - |\varphi|$, *for* $|\varphi| < 36°$ or $\sigma = 0$, *for* $|\varphi| \geq 36°$

φ is the latitude of the station.

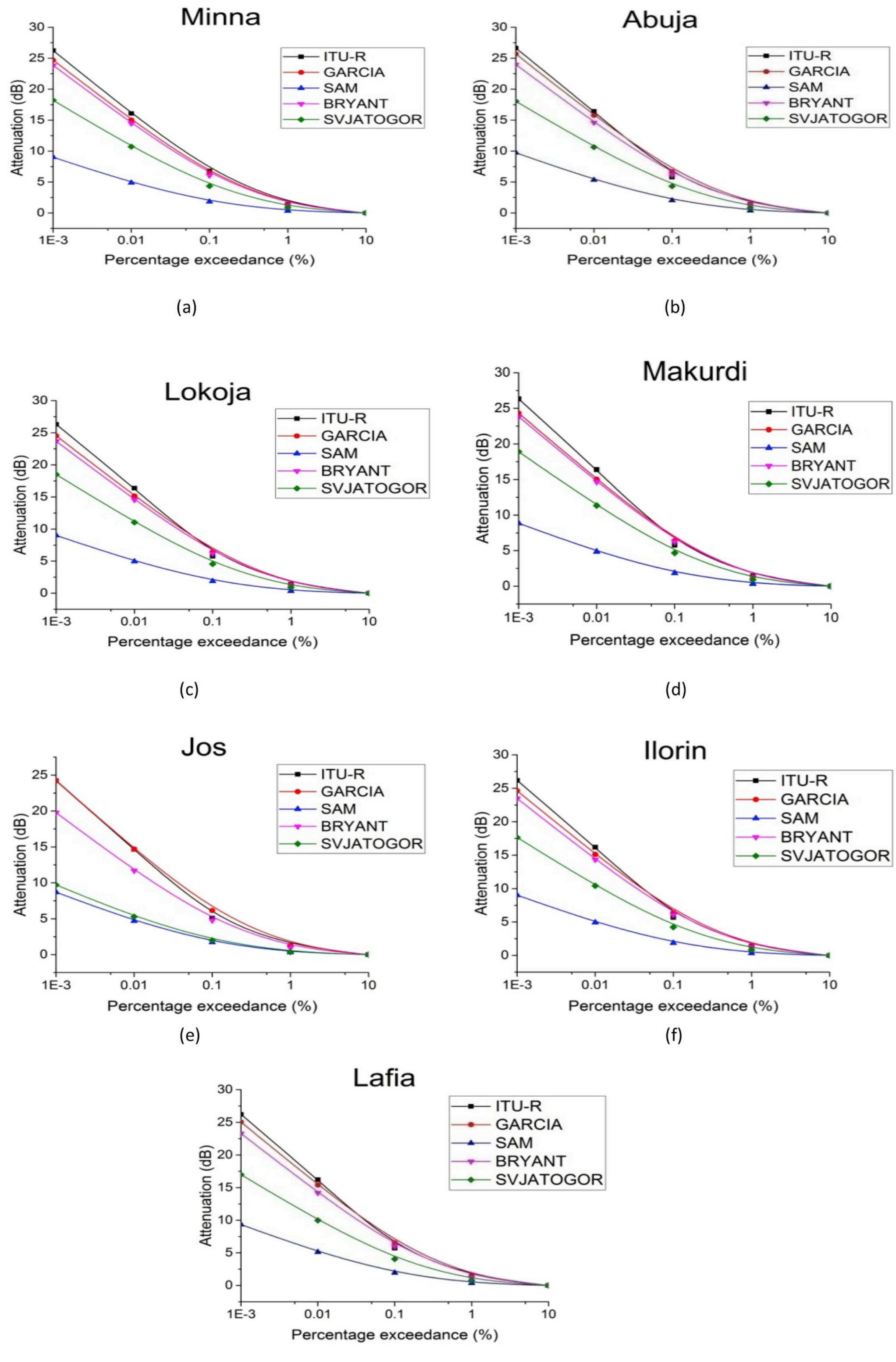

Fig. 4. Cumulative distribution of rain attenuation at 42.5° and Ku-band.

Step 8: The effective path length $L_{eff}(km)$ through rain is calculated as:

$$L_E = L_R v_{0.01} \tag{26}$$

Step 9: The predicted rain attenuation exceeded for 0.01% of an average year is obtained from:

$$A_{0.01} = \gamma_{R0.01} L_E \tag{27}$$

Step 10: The attenuation for other percentage exceedances are obtained using the expression below:

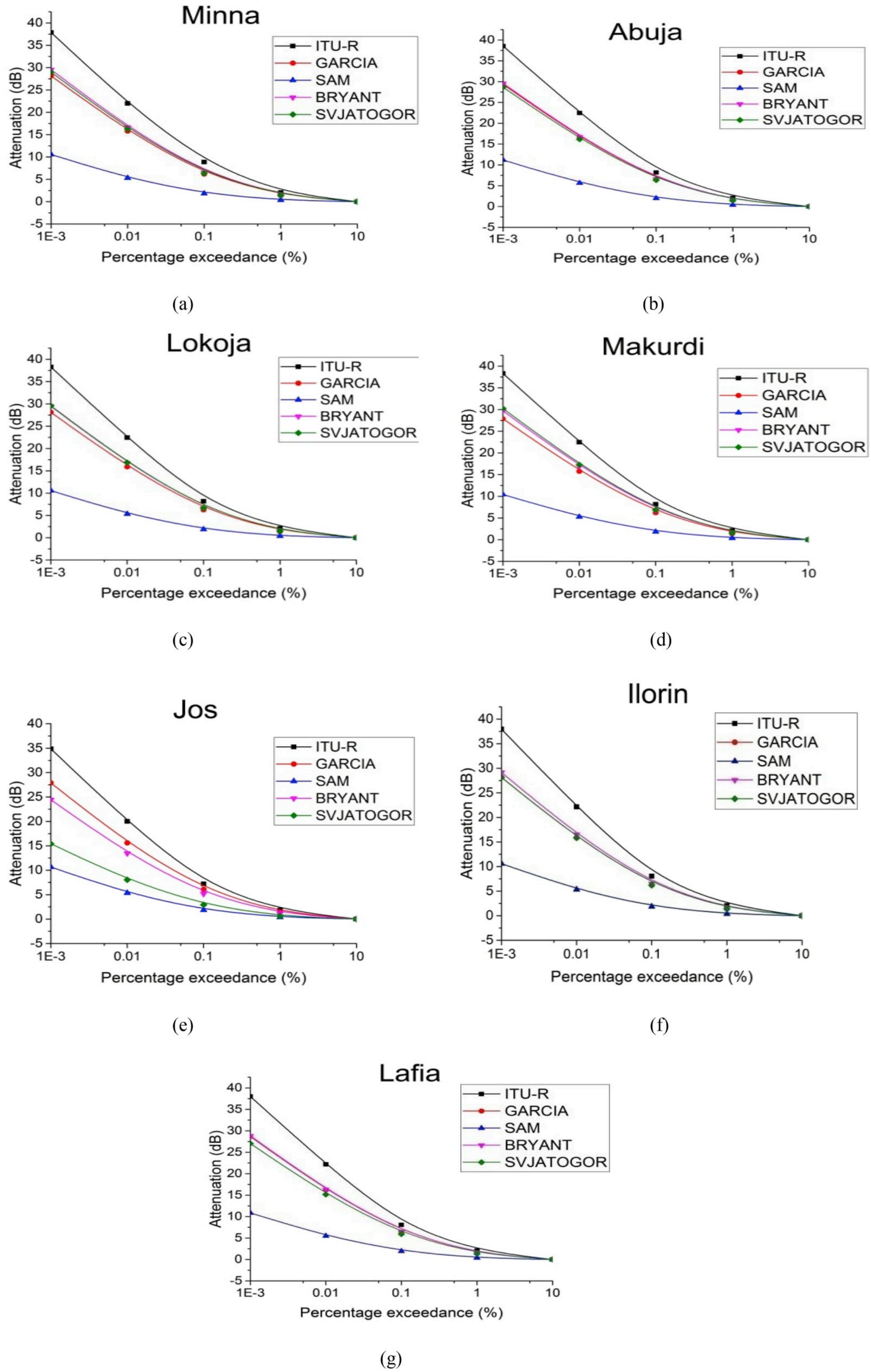

Fig. 5. Cumulative distribution of rain attenuation at 23° and Ku-band.

$$A_p(dB) = A_{0.01}\left(\frac{p}{0.01}\right)^{-[0.655+0.033\ln(p)-0.045\ln(A_{0.01})-z\sin\theta(1-p)]} \tag{28a}$$

where p is the percentage probability of interest, and z is given by

$$if\ p \geq 1\%,\quad z = 0 \tag{28b}$$

$$\text{if } p < 1\%,\ z = 0 \text{ for } \varphi \geq 36° \tag{28c}$$

$$z = -0.005(|\varphi| - 36)\ for\ \theta \geq 25°\ and\ |\varphi| < 36° \tag{28d}$$

$$z = -0.005(|\varphi| - 36) + 1.8 - 4.25\sin\theta,\ for\ \theta < 25°\ and\ |\varphi| < 36° \tag{28e}$$

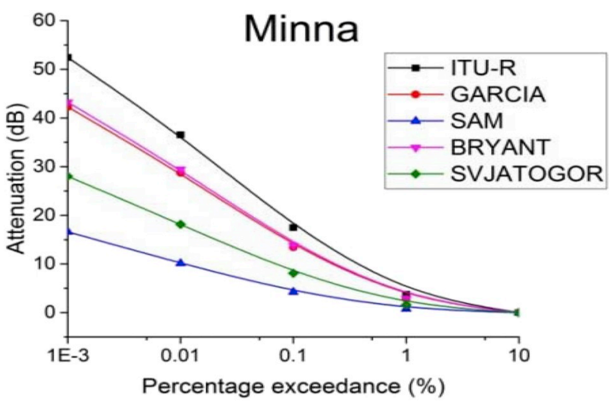

Fig. 6a. Cumulative distribution of rain attenuation at 55° and Ka-band.

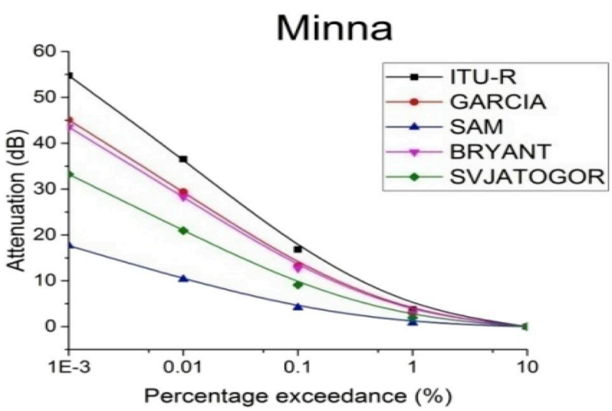

Fig. 6b. Cumulative distribution of rain attenuation at 42.5° and Ka-band.

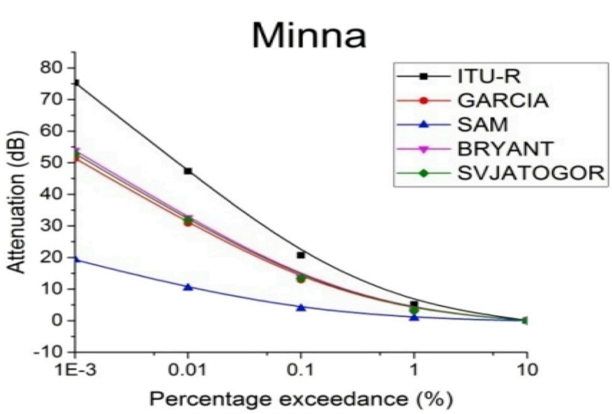

Fig. 6c. Cumulative distribution of rain attenuation at 23° and Ka-band.

3.3. The study area

The study area for this work is the North Central zone of Nigeria. This comprises six States: Niger (with Minna as the State capital), Nassarawa (with Lafia as the State capital), Kwara (with Ilorin as the State capital), Kogi (with Lokoja as State capital), Benue (with Makurdi as the State capital), Plateau (with Jos as the State capital); and the Federal Capital Territory (Abuja). The study area has a tropical climate with two distinct seasons: The dry season which prevails from November to March and the wet season which commences from April and ends in October every year. Fig. 1 shows the map of the study area.

The daily rainfall data used for this research work was acquired from the Nigerian Meteorological Agency (NIMET). The rainfall data was measured for a period of 33 years (January 1983 to December 2015) in the study area. The instrument employed for the data measurement is the Casella tipping bucket rain gauge.

4. Results and discussion

The rainfall analyses from the long-term daily rainfall data for the North Central States of Nigeria are presented. The data were collected for the period of 33 years (January 1983 to December 2015).

4.1. Rainfall distribution of the study area

The average monthly precipitation for 33 years for the study area is shown in Fig. 2. Only 15 years data were used for Lafia, Nassarawa State because the State is less than 33 years.

For the entire period, rainfall was generally low during the dry season (November–March) while the wet season (April–October) expectedly recorded higher amount of rainfall. Lokoja had the highest average precipitation of 107 mm in April while Jos recorded the highest amount in the months of May and June with 171 mm and 207 mm respectively. Abuja received the highest precipitation in July and August with values of 261 mm and 319 mm respectively. This is followed by Ilorin with 249 mm in September. In October, Abuja again recorded the highest precipitation of 158 mm. These months of observed peak rainfall are indicative of worst months of a radio link in the various locations (Ojo and Olurotimi, 2014). Also, the observed seasonal rainfall variation is attributed to the prevailing weather conditions in the area under study: During the dry season, the entire country is under the influence of dry continental air because of the dry and cold North-Easterly tropical continental (cT) air mass over the region (often accompanied by dust particles transported from the Sahara desert), which coincides with a period of minimum or no rain. In the wet season period, the deep moist maritime air predominates along with the characteristic heavy rainfall from the South-Westerly, tropical maritime (mT) air mass bringing moisture on to the country from the Southern hemisphere (Ojo, 1977).

The station characteristics including the average annual rainfall for 33 years and the computed point rainfall rate $R_{0.01}$ are given in Table 1.

4.2. Rain attenuation prediction

The point rainfall rate computation by Chebil model was used as initial input to predict the rain attenuation from the five rain attenuation models employed. The cumulative distributions of the rain-induced attenuation obtained at different percentages of time were compared for each of the stations. The frequencies used are 12.675 GHz for the Ku-band and 19.45 GHz for the Ka-band. Three elevation angles were considered: 55° which is the elevation angle of some satellite receivers over the Atlantic Ocean Region (AOR) in Nigeria, 23° which is the elevation angle over the Indian Ocean Region (IOR) and 42.5° which is the elevation angle of NIGCOMSAT-1R over the Atlantic Ocean Region.

The ITU-R model is the most widely accepted method for estimation of rain attenuation on satellite communication systems all over the world. Hence developed models are compared with it for reliability, especially when measured data are not available (Abayomi and Khamis, 2012). Results from experimental data have shown that the ITU-R rain attenuation prediction model which was derived based on lognormal distribution agrees closely with measured values (Choi et al., 1997; Emiliani et al., 2004; Mandeep and Allnut, 2007; Panchal and Joshi, 2016). As a result of this global acceptability of the ITU-R model, comparisons carried out in this work were based on the model.

Tables 2–4 show results for the computed geometric parameters relevant to satellite links at Ku and Ka frequency bands.

The cumulative distributions of the rain-induced attenuation obtained for the Ku-band at 55° elevation angle for the seven stations using the different attenuation models were compared. Fig. 3(a)–(g) show the result of the comparison for each of the stations.

As shown in Fig. 3(a)–(g), the Garcia-Lopez and Bryant models predicted closely with the ITU-R model, while the SAM and Svjatogor models underestimated the predicted rain attenuation values. For instance, the rain attenuation predicted by the ITU-R model for 0.001% exceedance probability is 25 dB for Minna, Abuja, Lokoja, Makurdi, Ilorin and Lafia, while it is 23 dB for Jos. At this same percentage of time, Garcia-Lopez model predicted 23 dB for Minna, Lokoja, Makurdi, Ilorin, Jos, Lafia and 24 dB for Abuja, while Bryant model predicted 24 dB for Minna, Abuja, Makurdi, 23 dB for Lokoja, Ilorin, Lafia and 20 dB for Jos. At 0.01%, the ITU-R model predicted 16 dB for all the stations except for Jos that had 14 dB. The corresponding attenuation predicted by Garcia-Lopez model is 15 dB for the other stations and 14 dB for Jos, while Bryant model predicted 15 dB for every other station except for Jos that recorded 12 dB. The predictions from the other two models, the SAM and the Svjatogor model were much lower as they underestimated the rain attenuation at the exceedance percentage of time considered in all the stations.

The cumulative distribution of the rain-induced attenuation at Ku-band was also examined at 42.5° elevation angle. The results are presented in Fig. 4(a)–(g).

As observed in Fig. 4(a)–(g), attenuation values are slightly higher at this elevation angle than at 55° for all the models and at all the stations. The difference is between 1 and 2 dB for $0.001\% \leq p \leq 1\%$. The trend observed in all the models at 55° elevation angle is also noticed here. The Garcia-Lopez and Bryant models still predicted closely with the ITU-R model (with the exception of Jos station), while the SAM and the Svjatogor model underestimated the attenuation.

Fig. 5(a)–(g) show the cumulative distribution of the rain induced attenuation for Ku-band at elevation angle of 23°.

It is observed from Fig. 5(a)–(g) that there is significant increase in the predicted rain attenuation. This is because of the longer path length in the rain region at this lower elevation angle. Therefore, these high attenuation values imply that satellite links over the Indian Ocean region (IOR) will suffer more rain attenuation than the ones linked to the Atlantic Ocean region (AOR). It can also be observed that at this elevation angle, none of the models predicted closely with the ITU-R, though the Garcia-Lopez, Bryant and Svjatogor models predicted close values with one another (except for Jos station).

Further comparisons of the cumulative distribution of rain-induced attenuation at Ka-band were made for the models at elevation angles of 55°, 42.5° and 23° for all the stations. The results obtained are presented in Fig. 6(a)–(c), though only results for Minna are presented here because of space constraint.

Fig. 6(a)–(c) show that rain attenuation at Ka-band is significantly higher than at Ku-band for all the elevation angles. The predicted rain attenuation by ITU-R model exceeded for 0.001% of the time is as high as 52 dB, 54 dB and 75 dB at 55°, 42.5° and 23° respectively. Also, at 0.01% of time, the rain attenuation predicted varies between 37 dB and 47 dB at the Ka-band frequency for the three elevation angles. Although, it is observed that none of the models predicted closely with the ITU-R model at the three elevation angles for the Ka-band, the values predicted by the Garcia-Lopez and the Bryant models were close to each other at 55° and 42.5° elevation angles (except at Jos station); the Garcia-Lopez, Bryant and Svjatogor models predicted close values with one another at 23° (except for Jos station also).

From the results obtained, it is evident that the ITU-R, Garcia-Lopez and the Bryant models can satisfactorily be used to predict rain attenuation at Ku-band, while the ITU-R model can conveniently predict rain attenuation at Ka-band in this region. The Svjatogor and Simple attenuation models are unsuitable for rain attenuation prediction in this region.

Also, the predicted attenuation values at 55° and 42.5° elevation angles at exceedance probability of 0.01% for the Ku band reveal that 99.99% availability (about 53 min outage in a year) of signal is possible at Ku band since attenuation values are < 20 dB, but there will be total fade out of signals at the Ka band during rainfall in all the stations since the predicted attenuation values are > 20 dB. This deduction is based on the fact that most satellites operating at 10 GHz and above are designed to withstand propagation losses that are ≤ 20 dB on its link because of limited carrier power at the output of the transmission amplifier which is about 150 W and minimal battery power onboard the spacecraft (Ippolito, 1986).

At 23° elevation angle, the values of attenuation predicted at 0.01% suggest that 99.99% availability of signal is impossible at both Ku and Ka bands in all the stations. In fact, it is not practicable at the Ka band because the transmitter power will have to be > 42 dB and 48 dB during rainfall to overcome rain losses. Therefore, there will be total fade out of signals in all the stations at Ka band for 99.99% availability.

5. Conclusion

The prediction of rain attenuation and its effects on satellite communication at Ku- and Ka-bands for the North Central region of Nigeria has been investigated for satellite links operating at 55°, 42.5° and 23° elevation angles. These predictions were made using five different rain attenuation models and the results obtained have shown that the ITU-R P.618 model, the Garcia-Lopez and the Bryant attenuation models are suitable for predicting rain attenuation at Ku-band, while the ITU-R model can be used to predict rain attenuation at Ka-band in this part of Nigeria. From the values of attenuation predicted at time percentage of 0.01% which is equivalent to 99.99% availability (about 53 min outage in a year), signal is possible at 55° and 42.5° elevation angles but impossible at 23° elevation angle at the Ku band. It is also impossible at the three elevation angles at the Ka band, thereby implying total signal fade out during rainfall events in all the stations.

Funding

This research did not receive any specific grant from funding agencies in the public, commercial or not-for-profit sectors.

Acknowledgements

The authors appreciate the Nigerian Meteorological Agency (NIMET) for making the acquisition of the rainfall data for this research possible.

Appendix A. Supplementary data

Supplementary data to this article can be found online at https://doi.org/10.1016/j.jastp.2019.03.005.

References

Abayomi, Y.I.O., Khamis, N.H.H., 2012. Rain attenuation modelling and mitigation in the tropics: brief review. Int. J. Electr. Comput. Eng. 2 (6), 748–757.
Ajayi, G.O., Feng, S., Radicella, S.M., Reddy, B.M., 1996. Handbook on Radio Propagation Related to Satellite Communication in Tropical and Subtropical Countries. ICTP, Trieste, Italy, pp. 7–14.
Bryant, G.H., Adimula, I., Riva, C., Brussard, G., 1999. Rain attenuation statistics from rain column, diameters and heights. Int. J. Satell. Commun. 19, 263–283.
Chebil, J., Rahman, T.A., 1999. Development of 1 min rain rate contour maps for microwave applications in Malaysia Peninsula. Electron. Lett. 35, 1712–1774.
Choi, Y.S., Lee, J.H., Kim, J.M., 1997. Rain Attenuation Measurements of the KoreaSat Beacon Signal on 12 GHz. CLIMPARA '98, Ottawa, Canada, pp. 208–211.
COST 225, 2002. Radiowave Propagation Modelling for SatCom Services at Ku-Band and above, Final Report. vol. 74. European Space Agency, the Netherlands, pp. 85–97 79.
Crane, R.K., 1978. A global model for rain attenuation prediction. EASCON Rec 391–395.
Crane, R.K., 1985. Evaluation of global and CCIR models for estimation of rain rate statistics. Radio Sci. 20 (4), 865–879.
Crane, R.K., 2003. Rain Attenuation Models: Attenuation by Clouds and Rain. Prop. Handbook for Wireless Commun. Sys. Design. CRC Press, USA, pp. 225–280.
Emiliani, L.D., Agudelo, E., Gutierrez, E., Restrepo, J., Fradique-Mendez, C., 2004. Development of rain-attenuation and rain-rate maps for satellite system design in the Ku- and Ka-bands in Columbia. IEEE Antennas Propag. Mag. 46 (6), 54–68.
Garcia-Lopez, J.A., Hernando, J.M., Selga, J., 1988. Simple rain attenuation method for satellite radio links. Year-to-year variability of rainfall for microwave applications in

the USA. IEEE Trans. Antennas Propag. 36 (3), 444–448.
Hossain, M.S., Islam, M.A., 2017. Estimation of rain attenuation at EHF bands for earth-to-satellite links in Bangladesh. In: Int. Conf. On Elect., Comp. and Commun. Eng. (ECCE), Cox's Bazar, Bangladesh, pp. 589–593.
Ippolito, I.J., 1986. Radiowave Propagation in Satellite Communications. Van Nostrand Reinhold Company Publishers, New York.
ITU-R, 2005. Specific Attenuation Model for Rain for Use in Prediction Methods. Rec. P.838-3, ITU-R P Sers. Int. Telecomm, Union, Geneva.
ITU-R, 2007. Propagation Data and Prediction Methods Required for the Design of Earth–Space Telecommunication Systems. Rec. P.618-9, ITU-R P Sers. (Int).
Kestwal, M.C., Joshi, S., Garia, L.S., 2014. Prediction of rain attenuation and impact of rain in wave propagation at microwave frequency for tropical region (Uttarakhand, India). Int. J. of Microw. Sci. and Tech. 1–6.
Mandeep, J.S., 2004. Comparison of one minute rainfall rate distributions for tropical and equatorial climates. Space Commun. 19, 193–198.
Mandeep, J.S., Allnut, J.E., 2007. Rain attenuation predictions at ku-band in South east asia countries. Prog. in Electromagn. Res., PIERS 76, 65–74.
Mandeep, J.S., 2011. Comparison of rain rate models for equatorial climate in South East Asia. Geofizika 28, 265–274.
Moupfouma, F., 1984. Improvement of a rain attenuation prediction method for terrestrial microwave links. IEEE Trans. Antennas Propag. 32 (12), 1368–1372.
Moupfouma, F., Martin, L., 1995. Modelling of the rainfall rate cumulative distribution for the design of satellite and terrestrial communication systems. Int. J. Satell. Commun. 13 (2), 105–115.
Obiyemi, O.O., Ibiyemi, T.S., Akande, S.O., 2014. Rainfall variability and impact on communication infrastructure in Nigeria. Jpn. Telecom. 25 (1), 6–11.
Ojo, O., 1977. The Climate of West Africa. Heineman, London, pp. 60–72.
Ojo, J.S., Ajewole, M.O., Sarkar, S.K., 2008. Rain rate and rain attenuation prediction for satellite communication in Ku and Ka bands over Nigeria. Prog. in Electromagn. Res. B 5, 207–223.
Ojo, J.S., Ajewole, M.O., Emiliani, L.D., 2009. One-minute rain rate contour maps for microwave-communication-system planning in a tropical country: Nigeria. IEEE Antennas Propag. Mag. 51, 82–89.
Ojo, J.S., Olurotimi, E.O., 2014. Tropical rainfall structure characterization over two stations in Southwestern Nigeria for radiowave propagation purposes. J. Emerg. Trends Eng. Appl. Sci. 5 (2), 116–122.
Panchal, P., Joshi, R., 2016. Performance analysis and simulation of rain attenuation models at 12-40 GHz band for an earth space path over Indian cities. 7th Int. Conf. on Commun., Computing and Virtualization, ScienceDirect 79, 801–808.
Ramachandran, V., Kumar, V., 2005. Invariance of accumulation time factor of Ku-band signals in the tropics. J. Electromagn. Waves Appl. 19 (11), 1501–1509.
Rice, P., Holmberg, N., 1973. Cumulative time statistics of surface-point rainfall rates. IEEE Trans. Commun. COM- 21, 1131–1136.
Salonen, E.T., Poiares-Baptista, J.P.V., 1997. A new global rainfall rate model. In: Proc. Of 10th Int. Conf. on Ant. and Propag., Pub N 14-176-436, pp. 182–185.
Segal, B., 1986. The influence of rain gauge integration time on measured rainfall-intensity distribution functions. J. Atmos. Ocean. Technol. 3, 662–671.
Shrestha, S., Park, J., Choi, D., 2016. Rain rate modeling of 1-min from various integration times in South Korea. SpringerPlus 5 (433), 1–34.
Shrestha, S., Choi, D., 2017. Characterization of rain specific attenuation and frequency scaling method for satellite communication in South Korea. Int. J. Antennas Propag. 1–16.
Shrestha, S., Choi, D., 2018. Diurnal and monthly variations of rain rate and rain attenuation on Ka-band satellite communication in South Korea. Prog. In Electromagn. Res. B 80, 151–171.
Stutzman, W.L., Dishman, W.K., 1984. Correction to a simple model for the estimation of rain-induced attenuation along earth-space paths at millimeter wavelengths. Radio Sci. 19, 946.
Sujimol, M.R., Acharya, R., Singh, G., Gupta, R.V., 2015. Rain attenuation using Ka and Ku band frequency beacons at Delhi earth station. Indian J. Radio Space Phys. 44, 45–50.
Svjatogor, L., 1985. Prostranstvennaia korelacia vypadenjija dozdjej vdol zemnoj poverchnostji (in Russian). In: Symposium Expertov Stran Uchastnic Programmy INTERKOSMOS (Interkosmos Symposium, Theme 5 of the Established Telecommunication Working Group, Dresden, GDR).
Tamosiunaite, M., Tamosiuniene, M., Gruodis, A., Tamosiunas, S., 2010. Prediction of electromagnetic wave attenuation due to water in the atmosphere. 1. Attenuation due to rain. Innov. Infotech. for Sci, Business and Edu. 2 (9), 3–10 2029–1035.
Watson, P.A., Sathiaseelan, V., Potter, B., 1981. Development of a climatic map of rainfall attenuation for Europe. Postgrad. Sch. of Elect. and Electron. Eng., Univ. of Bradford, U.K. 300, 134.